Chapter 9
Bioactive Glasses in Angiogenesis and Wound Healing: Soft Tissue Repair

Gurbinder Kaur

Bioactive glasses have shown immense potential in the field of orthopedics and dental applications. Many research articles have been published over years based on the tissue engineering and orthopedic/bone regeneration capabilities of bioactive glasses. Due to high osteoconductive and osteostimulative properties of bioactive materials, they are the most preferred biomaterials. Bioactive glasses have the ability to bond directly to the bone, thereby extending its interaction with soft tissues as well. After the discovery of 45S5 Bioglass®, the biomaterial world was revolutionized [45S5 Bioglass® composition is known as the grandfather composition]. After bioglass, other two compositions, which received wide attention, are 13-93 and S53P4 compositions due to their excellent clinical outcomes. Apart from the bone and tissue regeneration, glasses have been studied for the soft tissue repair, angiogenesis, and wound repair capabilities as well.

9.1 Bioactive Glass and Soft Tissue Interaction

When bioactive glass (BG) comes in contact with the physiological fluids, then a series of ion dissolution and precipitation reactions occur on the surface of BG. These set of reactions cause change in pH and HAp layer formation. Upon implantation of bioactive glasses in body, two types of interactions occur, i.e., intracellular and intracellular (Fig. 9.1).

It must be noted that the functional material and structural properties of components of cell adhesion and physicochemical parameters are determined by the surface topography. Moreover, the composition of BG plays a crucial role in determining the interaction mechanism. The pH of ions and progenitor cell populations determine the rate of regeneration and degree of bonding mechanism. For the interaction of soft tissues and BG, long-time interfacial bonding without inflammatory response and rapid interfacial layer formation governed by

G. Kaur, *Bioactive Glasses*, Series in BioEngineering,
DOI 10.1007/978-3-319-45716-1_9

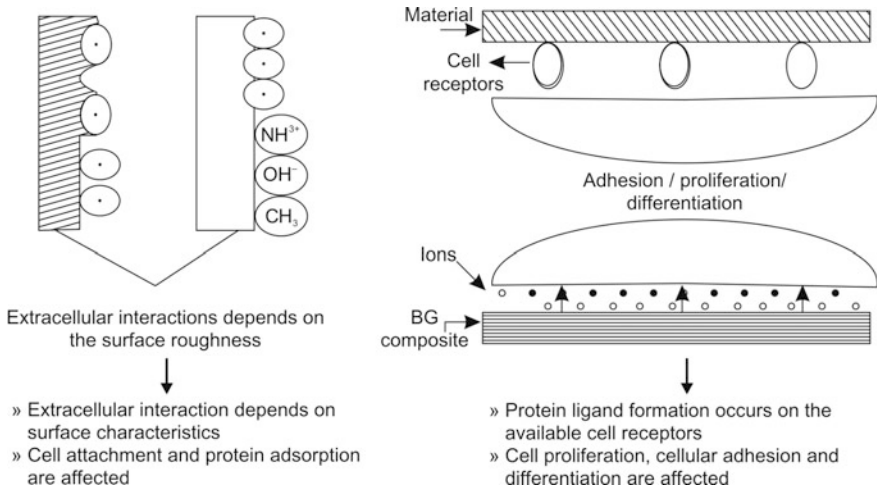

Fig. 9.1 Effect of the cell interactions on the tissues

extracellular cell matrix shall take place. Additionally, stress transfer gradient is required across the interface in order to avoid cell signaling for either tissue or implant resorption.

9.2 Applications of Soft Tissue Repair

Hard–soft tissue interfaces, particularly in BG/polymer composite, are investigated widely and furthermore, the surface modification of BGs is carried out to enhance their bioactivity/biocompatibility. Due to the 'hard' physical characteristics of BG, hard tissue interaction has been studied and less attention has been paid to the soft tissue interaction. Wilson and coworkers have performed wide in vivo and in vitro experiments to study the Bioglass® cytocompatibility and toxicity, when in contact with various soft tissues.

Bioactive glasses such as 45S5, 45S5F, and 52S4.6 have been used for in vitro investigations on hamsters, chickens, mice and rats, whereas dish-shaped BG were implanted subcutaneously and intramuscularly in the peritoneal cavity of mammals (like dogs). The results indicated tissue growth and adhesion around the implants, and the autopsy result indicated no inflammatory response of the host tissue. Gatti and coworkers implanted glass granules of size ~ 300 μm, in the dorsal muscle and under dorsal skin of rabbits. In addition to this, the defects were created surgically in the sheep jaw, and glass granules were implanted into them to understand the hard/soft tissues interaction with glass. After 2-month and 3-month excision in rabbits and sheep, respectively, it could be seen that the BG granules and their surroundings exhibited almost similar morphology, indicating that the nature of

reactions is independent of the implantation site and tissue type. Though the literature reports extensive study on bioactive glasses and other biomaterials (metallic implants, polymers, polymer/bioactive glass composites), sporadic studies are available on the bioglass in soft tissue applications, such as angiogenesis and wound healing. The prime focus of this chapter would be to list all these applications one by one.

9.3 Bioactive Glass in Angiogenesis

Angiogenesis is the mechanism of formation of new blood levels from the preexisting one. Angiogenesis is vital for granulation tissue formation and the wound healing mechanism. Various growth factors such as vascular endothelial growth factor (VEGF), TGF-β, and fibroblast growth faction (FGF) regulate angiogenesis. VEGF increases the capillary numbers in given site and hence acts as a major contributor to the angiogenesis. Due to increased blood flow at the affected area, VEGF is unregulated with muscle contraction causing increased mRNA production of VEGF receptors. Matrix metallic proteinase (MMP) inhibition prevents the formation of new capillaries because they degrade the protein, which keeps the vessels walls strong, thereby allowing the endothelial cells to escape into interstitial matrix, resulting in sprouting angiogenesis.

For the regeneration process to occur, neurovascularization is an essential criterion so that the growing cells are with provided oxygen and nutrients. Hence, the angiogenic potential of bioactive materials is receiving attention for the tissue engineering application. Angiogenesis is a process that can take place during normal tissue regeneration as well as during the pathogenic conditions such as malignant tumors/cancer. Angiogenesis form the basis of tissue engineering, and hence the mass transport and oxygenation mechanics are to be regulated.

Gorustovich and coworkers provided a broad review of the in vitro/in vivo effects of glasses on the angiogenesis listing experimental evidences. Keshaw and coworkers studied angiogenic growth factor release from the cells encapsulated in alginate beads with bioactive glass. Alginic acid was derived from the *macrocystis pyrifera,* and 45S5 Bioglass® was used for the CCD-18Co normal colon fibroblast human cells. The alginate beads containing 0.01 and 0.1 % 45S5 Bioglass® released higher VEGF after 3, 6, 9, and 17 days postencapsulation. VEGF is endothelial cell-specific mitogen and is involved in pathological and physiological angiogenesis. For the same concentrations, fibroblasts culture revealed an increase in the bioactive glass-coated surfaces. For the alginate beads containing 0.1 % 45S5 Bioglass®, significant increase in the endothelial cells is observed attributed to the presence of VEGF and other angiogenic factors in optimum concentration.

It must be noted that the concentration of 45S5 Bioglass® shall be optimized, i.e., if 45S5 Bioglass® content is quite high, then VEGF secretion reduces, most likely due to the cytotoxic effects. The alginate beads containing 0.01–0.1 % 45S5

Bioglass® lysed with EDTA, yielded high VEGF as compared to the beads with 0–1 % 45S5 Bioglass® glass. Day found the stimulation of angiogenesis and angiogenic growth facture using bioactive glass 45S5. For the 45S5 Bioglass® coating of 0.03125–0.625 mg/cm^2 in tissue culture wells with human intestinal fibroblasts, enhanced amount of VEGF could be observed. To assess the effect of growth factors secreted from fibroblasts in response to 45S5 Bioglass® on angiogenesis, an in vitro model of human angiogenesis was used. It was observed that 45S5 Bioglass® stimulates fibroblasts to secrete growth factors thereby causing a significant increase in angiogenesis. Significant increase in the endothelial tubules number and number of tubule junctions could be observed within the conditioned media obtained from fibroblasts cultured on the 45S5 Bioglass®. The number of endothelial tubules, tubule length, and tubule junctions were reduced as compared to controlled endothelial cells due to the presence of 20 μM suramin, an angiogenesis inhibitor (Fig. 9.2).

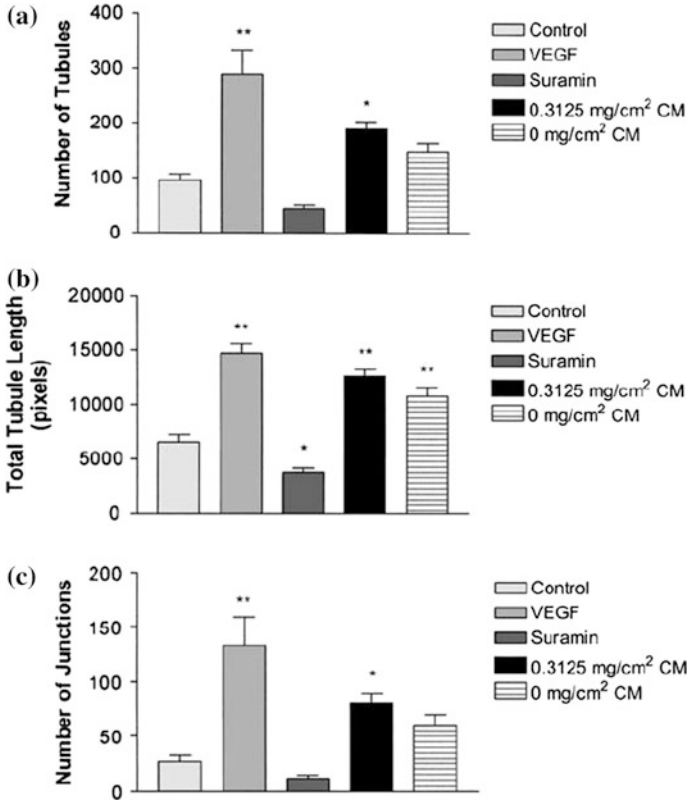

Fig. 9.2 **a** Number of tubules; **b** total tubule length; **c** number of junctions formed in the conditioned medium, produced by CCD-18Co fibroblasts grown on Bioglass® at 0.3125 mg/cm^2, or in medium without Bioglass®, on angiogenesis in vitro (Day 2005)

The studies carried out by Day also demonstrated that small quantities of bioglass could stimulate the expression of VEGF and hence enhance in vitro angiogenesis, though it is not clear whether other angiostatic factor is also released. Complex network of interconnected tubules and tubule branching could be seen in addition to fibroblast-conditioned medium produced in 45S5 Bioglass® presence (in vitro). These tubules mimic the essential stages for the angiogenesis, involving cell migration, proliferation, anastomosis, and vessel branching.

Leach and coworkers coated VEGF-secreting polymeric scaffolds with the 45S5 Bioglass® (45 % SiO_2, 24.4 % $N9_2O$, 24.6 % CaO, 6 % P_2O_5). VEGF enhances osteoconductivity via biomineralization, and localized VEGF delivery has been beneficial for bone regeneration as the neurovascularization osteoblast migration and bone turnover are promoted. The porous scaffolds were poly (lactide-co-glycolide) for the localized protein delivery, and then the surface was coated with 45S5 Bioglass® (up to 0.5 ± 0.2 mg of BG could be deposited). Mitogenic effect could be observed on the human micro-vascular endothelial cells (HMVEC) by the VEGF released from BG-coated and non-coated scaffolds. Though after day 6, the BG-coated blank scaffolds could support enhanced HMVEC proliferation, but not detectable by day 9, probably due to complete dissolution of the material. After 10 days, the proliferation values decreased for VEGF-releasing scaffolds along with mitogenicity comparable to VEGF-secreting uncoated scaffold. It suggests that with the material degradation, the BG coating contribution is degrading upon seeding the scaffolds with HMSCs and differences in alkaline phosphatase activity could not be observed between scaffolds at different time points. The BG-coated scaffolds were implanted in cranial defects of Lewis rats. VEGF-releasing BG (BGV) depicted higher neurovascularization in the defect (117 ± 20 vessel/cm^2) as compared to BG-coated scaffolds (66 ± 8 vessel/cm^2).

Figure 9.3 reveals higher vascularization and angiogenic capacity in BG-coated scaffolds. Robust angiogenic response could be seen by the coated scaffolds lacking VEGF, in the studies conducted on similar model by Murphy and coworkers. Bone mineral density results indicated that the prolonged VEGF delivery from polymeric substrates improved the maturation of newly formed bone. With BGV scaffolds, a slight increase in the newly formed bone within the defect could be seen as compared to BG-coated scaffolds.

Day and coworkers assessed the effect of 45S5 Bioglass® on VEGF secretion using a rat fibroblast cell line (208F). Enzyme-linked immunosorbent assay (ELISA) of media collected from the fibroblasts grown for 24 h on 45S5 Bioglass® particles-coated surface [via a suspension of 45S5 Bioglass® in distilled and deionized water) yielded increased VEGF concentration. The same group conducted similar studies on PLGA disks containing different concentrations of Bioglass® with particle size <5 μm. Increased VEGF secretion is observed upon culturing fibroblasts L929 on PLGA disks with 0.01–1 % 45S5 Bioglass® particles. The results of Day and Keshaw revealed that endothelial cell proliferation was increased by conditioned medium collected capable of inducing proliferation. However, for the bovine aortic endothelial cells (BAEC), plated on zinc-doped 45S5 bioactive glasses, significantly higher bovine aortic endothelial cells could be

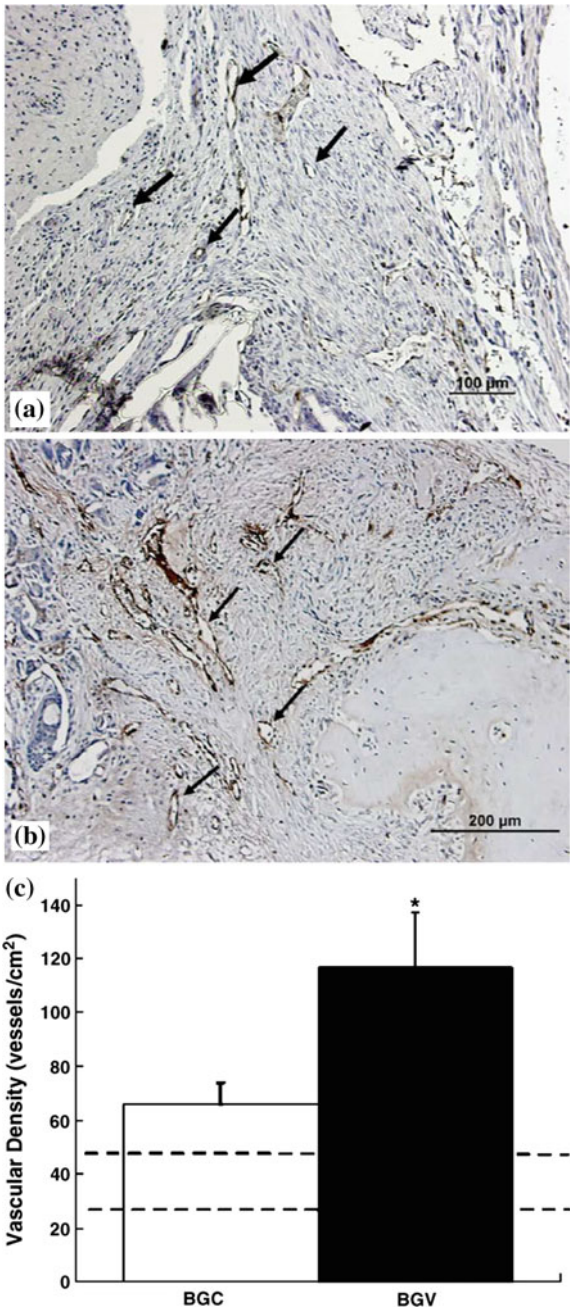

Fig. 9.3 Staining for vWF of decalcified tissues treated with **a** BGC scaffolds and **b** BGV scaffolds, at 2 weeks. *Arrows* denote circular vessels are visible in both samples. **c** Quantitative analysis of vessels in each study group (Leach et al. 2006)

seen on 5 % ZnO-containing glasses as compared to 20 % ZnO-containing glasses and control 45S5 glass. The high rate of dissolution for the 20 % ZnO-containing glasses causes pH changes and hence affects the cell proliferation.

Leu and coworkers found a dose-related proliferative response of endothelial cells cultured with Bioglass®-loaded collagen toward the soluble products of the constructs. The collagen sponges loaded with 1.2 mg Bioglass® particles yielded highest proliferative response, whereas considerable inhibition of endothelial cell proliferation could be observed with the sponges with highest bioglass content of 12 mg. In addition to this, the endothelial cells exposed to 1.2 and 0.12 mg Bioglass® demonstrated higher VEGF mRNA secretion after 72 h of exposure.

Leu and coworkers also explored the proangiogenic potential of 45S5 Bioglass® by exploring its tubule-generating ability within coculture of endothelial cells and fibroblasts. The stimulation of cocultures was performed with conditioned medium from 45S5 Bioglass®-treated rat aortic rings, and like endothelial proliferation assays and dose-related tubule formation response of Bioglass® could be seen. For the 1.2 mg 45S5 Bioglass®, highest number of tubules could be seen, whereas for 6, 0.12, and 0.6 mg Bioglass®-loaded sponges, no tubule formation over the collagen sponges could be seen.

Durand and coworkers studied the angiogenic effects of ionic dissolution products released from boron-doped 45S5 bioactive glass [45S5.2B: 45 % SiO_2, 24.5 % Na_2O, 24.5 % CaO, 6 % P_2O_5 and 2 % B_2O_3]. 45S5.2B composition is also reported to enhance the bone formation upon implantation into the intramedullary canal of the rat tibiae. In addition to this, the human umbilical vein endothelial cells (HUVECs) possess greater migratory and proliferative response, enhanced secretion of proangiogenic cytokines (IL-6 and bfGF), and higher tubule formation capacity, upon stimulation from the ionic dissolution products. The ELISA test carried out to determine the endogenous levels of integrin α_v β_3 in chorioallantoic membrane (CAM) of quail embryos revealed that upon treatment (2 days) with ionic dissolution products from bioactive glass 45S5.2B, the levels of expression are 2.5- to 3-fold higher than those treated with Hank's balanced salt solution (HBSS). Moreover, greater expression of β_3 subunit of integrin α_v β_3 was seen in the Western blot test.

As for as the vascular density results are concerned, no significant differences of CAM treated with HBSS + 45S5.2B/bFGF or HBSS + 45S5.2B for the vascular density could be observed when compared to negative control (HBSS) even after five days of treatment (Fig. 9.4).

Anyhow, for the CAM treated with 4BSS + 45S5.2B and 4BSS + 45S5.2B/bFGF, higher vascular density of 30 and 73 % is observed, respectively, which is comparable to the response observed with HBSS + bFGF. The authors further investigated the effect of boron concentration on the angiogenic activity in the CAM treated with HBSS enriched with the 45S5.2B dissolution product. For the boron concentrations of 5, 50, and 150 μM, the corresponding CAM yielded greater vascular density as compared to the control HBSS after 5 days of treatment (Fig. 9.5).

For the HBSS containing 50 or 150 μM borate, no significant differences in the angiogenic response could be seen after 2 or 5 days of treatment. The studies of Durand and coworkers confirmed that the ionic dissolution products did not induce any angiogenic response and hence did not affect the normal development of the

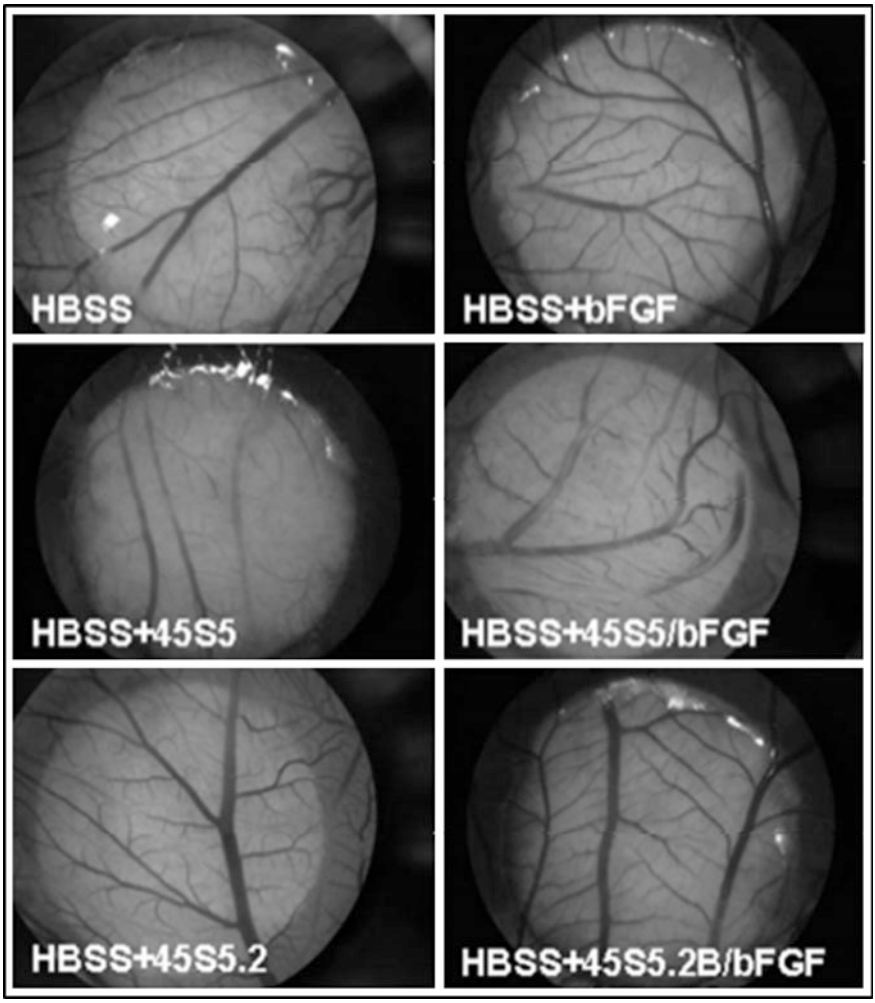

Fig. 9.4 The angiogenic response of CAM, five days posttreatment (Durand et al. 2014)

embryonic quail CAMs' vasculature. This could be due to the smaller contact area of CAM with the scaffolds causing insufficient ion release. Boron in the form of H_3BO_3 activates the mitogen-activated protein kinase (MAPK) signaling pathway to enhance cell proliferation and growth at low concentrations and inhibiting them at higher concentrations. Angiogenesis involves vascular growth factors and extracellular matrix interacting molecules like integrins. α_v β_3, a heterodimer integrin, is expressed at low levels on quiescent endothelial cells in vivo but is upregulated during vascular remodeling and angiogenesis. Lin and coworkers

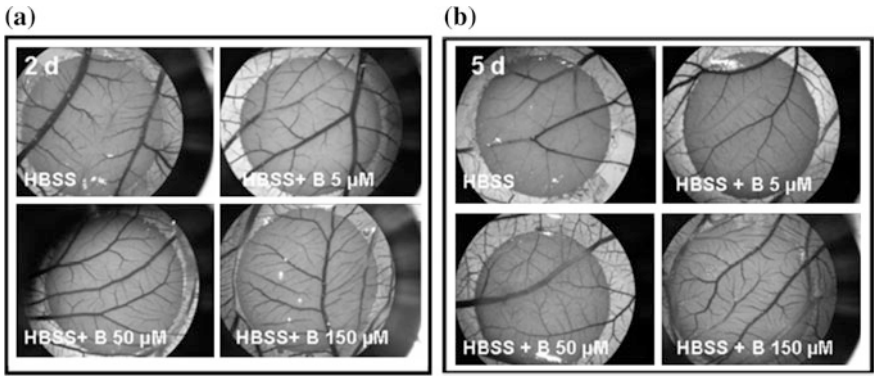

Fig. 9.5 **a** 2-day and **b** 5-day angiogenic response after treatment with HBSS and different borate concentrations (Durand et al. 2014)

demonstrated that no systemic cytotoxicity could be observed upon subcutaneous implantation of 13-93B3 glass (53 wt% B_2O_3) microfibers in rats, even when high amount of glass up to 1120 mg/animal was used. The controlled release of borate ions could represent promising alternative for the neurovascularization in regenerative medicine.

Mahmood and coworkers demonstrated the relation between glass porous matrix and in vivo vascularization. A fiber-based bioactive glass was used with composition of 32.24 % CaO, 9.26 % P_2O_5, 41 % SiO_2, and 17.5 % Al_2O_3 with recombinant human bone morphogenetic protein–2 (rhBMP–2). Vascularization was evaluated by mRNA expression of KDR and Flt-1, two VEGF receptors.

The scaffolds were designed in two shapes, i.e., bundle shape and porous ball constructs. The receptors KDR and Flt-1 did not express for the subcutaneously implanted bundle-shaped scaffolds in rats, 2–4 weeks postimplantation, but the same receptors expressed in porous ball scaffolds under same conditions. The histology results also revealed that after 2–4 weeks of subcutaneous implantation of scaffolds, higher bone formation could be seen for porous ball constructs compared to the bundle-shaped scaffolds. rhBMP promotes vascularization and also induces bone formation.

Ghosh and coworkers evaluated the biological response of BG block with the composition of 43.7 SiO_2, 19.2 % CaO, 5.46 % P_2O_5, 9.4 % B_2O_3, and 22.24 % Na_2O upon implantation in the radius bone of Bengal goats. After 3-month implantation, a well-formed vascularization and bone tissue ingrowth, directly integrating with the neighboring bone, could be seen. The same group worked on the same experimental model with glass composition of 58.6 SiO_2, 23.66 % CaO, 3.38 % P_2O_5, 3.78 % B_2O_3, 1.26 % TiO_2, and 9.32 % Na_2O, and found the establishment of vascular supply and well-organized transimplant angiogenesis across the bone defects.

Andrade and coworkers evaluated the angiogenic and inflammatory response of BG-coated collagen scaffolds upon subcutaneous implantation in mice. It was observed that the hemoglobin (Hb) content extracted from implants is higher in glass-coated collagen implants compared to glass-free group, after 14 days of implantation. No inflammatory response associated with the glass-coated collagen samples could be observed for in the presence of Hb, as revealed by the control group. Gerhardt and coworkers investigated the angiogenic effect of BG by comparing composite PDLLA/BG scaffolds with plain poly (D, L Lactide) (PDLLA) and obtained marked increase in the VEGF release by fibroblasts cultured on PDLLA/BG composites compared to plain PDLLA films. The in vivo experiments on a rat model confirmed enhanced vascularization and higher percentage of blood vessel formation, as shown by the stereological examination.

9.4 Phases in Wound Healing

Whenever the skin breaks, muscle tear or the burns occur; then, the tissue integrity is compromised, resulting in wounds. The phases of wound healing involve the following:

(a) Barrier protection: The wound shall be protected from the external environments by applying dressing and hydrogen. Hydrogels provide soothing barrier, which help in insulating the wounds against hot and cold stimuli along with acting as cushion against external physical conditions such as temperature and pressure of touch.
(b) Inflammatory Phase: The body responses naturally during this phase. After the occurrence of wounding, the clot formation would occur due to contraction of blood vessels in the wound bed. Upon stoppage of bleeding or hemostasis, the dilation of blood vessel occurs to allow growth factors, enzymes, antibodies, white blood cells, and nutrients to reach the wound site. Changes in vascular phase may cause inflammation, which is normal and prerequisite of healing. Injured tissue can cause histamine release causing blood vessels to dilate (vasodilation), resulting in blood exudation creating hot, swollen, reddened, and painful area around the wound. Near to the wound, the white blood cells adhere to the dilated endothelial walls. The phagocytosis also occurs, which is a cellular process of engulfing solid particles by the cell membrane to yield a phagosome known as food vacuole. Phagocytosis is very crucial step for the pathogen and cell debris removal. After few days, another phagocyte known as macrophage will predominate and stay in the wound until the inflammation ceases. The macrophages play dual role, i.e., to stimulate lymphocytes/immune cells to respond to the pathogen and to phagocytose cellular debris and pathogens. Usually, wound healing occurs without infection due to the

microbicidal capacity of macrophages. Another cell known as fibroblast start responding to the chemical signals released by the macrophages. Fibroblasts are well known for providing structural framework to many tissues and secrete the precursors for the extracellular matrix components.

(c) Proliferation/fibroblastic phase: Rebuilding follows, once the inflammatory phase is completed; fibroblasts are the building blocks of this phase. During this phase, the wound gets resurfaced and strength is imparted to it. Around blood vessel, loose tissues are present, containing mesenchymal cells that release fibroblasts. Another granulation tissue involved in this phase is comprised of collagen and extra cellular matrix (into which the blood network develops or angiogenesis occurs). During this phase, three processes, i.e., epithelialization, wound contraction, and collagen production, occur to achieve coalescence and closure of wounds. In addition to this, healthy granulation tissue depends on the fibroblast receiving healthy environment via adequate nutrient and oxygen supply. Healthy granular tissue possesses uneven texture and is red/pink in color. The undamaged epithelial cells at the wound margin start producing through mitosis, coursing a periphery formation around the wound. But in case the wound is extensive or it is a necrotic tissue, then the epithelial migration cannot proceed due to poor oxygen availability and dehiscence may occur. Dehiscence is the splitting or premature bursting of the wound. To facilitate epithelialization, moist dressings shall be done such as hydrogel dressings, which protect the wound from traumas.

The wound surface is closed by epithelialization, and then the contraction pulls the entire wound together causing defect shrinkage. A specialized cell known as myofibroblast is involved in the contraction process. Myofibroblast represents a cell that occurs in between smooth muscle cell and fibroblast during differentiation. Myofibroblasts attach to the skin margins and then pull entire epidermal layer inwards. The conclusive step during wound heating is collagen production by fibroblasts. To enhance fibrous tissue production, the adequate oxygen, (Zn, Fe, Cu) cofactors, nutrients, and ascorbic acid are required.

(d) Maturation/remodeling phase: During this phase, the wound has closed and collagen remodeling from type III to type I is involved. During this phase, reduction in cellular activity and blood vessels near the wounded area could be observed. The collagen synthesis occurs at a high rate, but no further increase in scar mass occurs. With the help of enzyme collagenase, the old collagen is broken down and new one is created to maintain the equilibrium, and this process continues until the remodeling ends depending upon the state and depth of injury. In case the process of healing does not take properly, then the keloid or hypertrophic scar could be formed due to the collagen overproduction. Keloids are rubbery firm lesions, which are shiny and benign in nature, whereas hypertrophic scar is raised as red lump over the injury. Figure 9.6 depicts all the stages of wound healing.

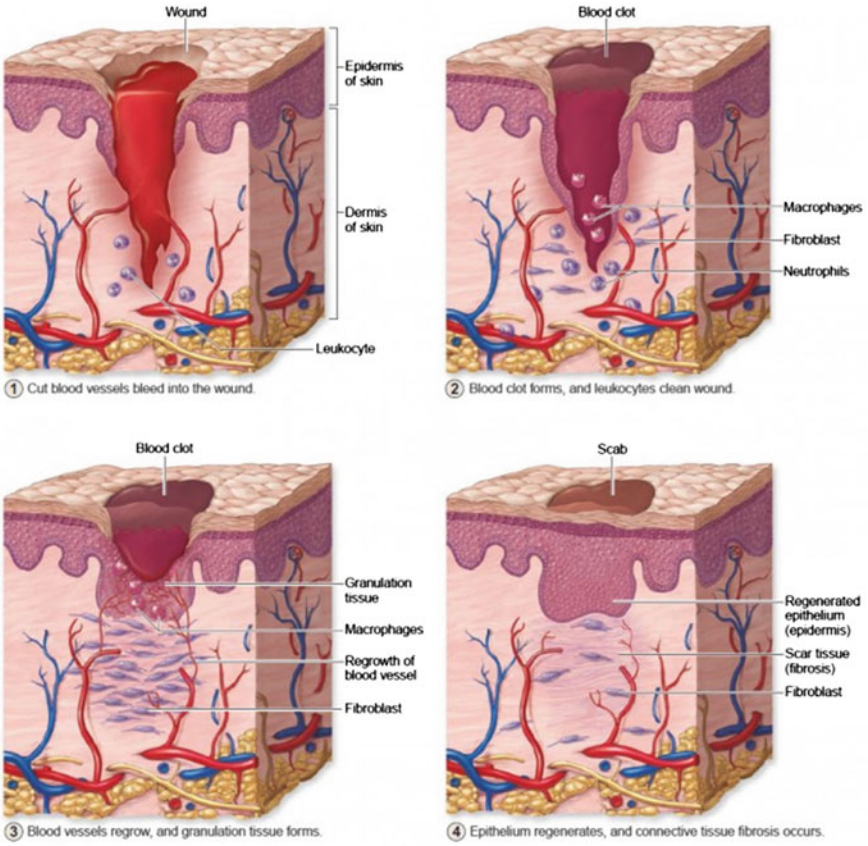

Fig. 9.6 Stages in wound healing (Photocourtesy by: Biology Forms)

9.5 Bioactive Glasses in Wound Healing

Ma and coworkers synthesized BG glass ceramics-based man fibrous membranes for the wound dressing [30 % SiO_2, 27 % CaO, 20 % B_2O_3, 4 % P_2O_5, 1.5 CuO, 1 % ZnO, 3 % K_2O, 9 % Na_2O, wt%] using electrospinning technique with varying chitosan: gelatin ratios (C/G ratio) (Fig. 9.7).

It is clear from the SEM observations that the G/C nanofibers are composed of open pores with several micron dimensions. As the C/G ratio increases from 1/19 to 5/15 in the solution, the presence of beads could be observed in the fiber body prone to aggregation. The sol-gel-derived glass is highly dispersible with nanoscale-dimensional size. The fiber morphology is changed with an increasing BG/(chitosan + gelatin) ratio, i.e., from 6 to 15 %, where the BG is introduced via electrospinning technique for C/G ratio of 3/17. As shown in Fig. 9.8, upon increasing the BG/(G+C) ratio to 15 %, the mats grow blade like continuous fibrous

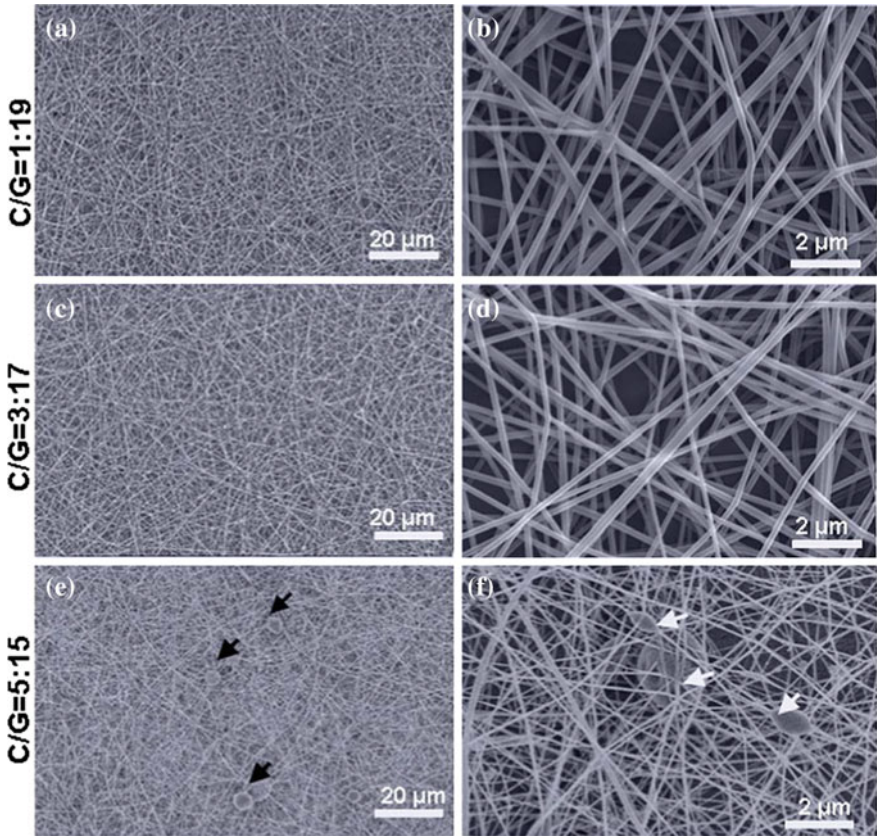

Fig. 9.7 SEM images of the G/C nanofibrous mats with different C/G mass ratios (Ma et al. 2014)

networks. The bioactive glass particles could be seen anchoring in the fiber matrix with scarce expose in porous network upon increasing BG content. BG-introduced mats exhibited high tensile strength, almost 2–4 folds higher than the pure organic mats. Upon addition of 15 % BG, the average elongation ratio of mats increased by 150 %, favoring it for the biomedical application. Collagen is one of the most abundant insoluble structural fibers inside the human body and is controlled hydrolysis yields gelatin. The gelatin temperature of human physiological fluid and gelatin is close to each other, which makes it necessary to cross-link the gelatin-based dressings carefully for improving the structural and thermal stabilities. The G/C–15 BG and G/C–0BG mats were subcutaneously implanted in rats, and it was observed that after 2 weeks of implantation, no inflammation or adverse response of the host tissue could be seen, indicating their high biocompatibility as depicted in Fig. 9.9. After 4 weeks of implantation, the degradation of the G/C-15 BG and G/C–0BG mats was observable. The bioactive potential of G/C–BG mats

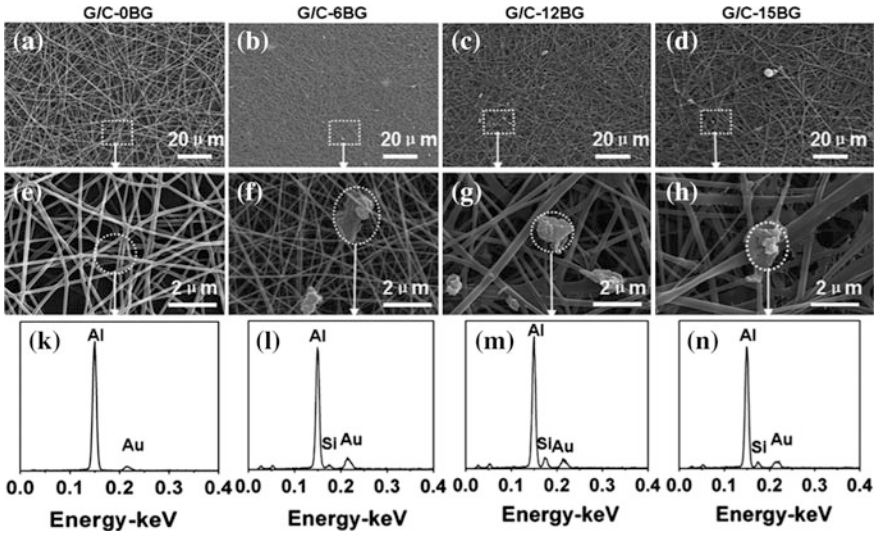

Fig. 9.8 (A-H) SEM observation and (K–N) EDX analysis of the G/C–xBG membranes with different amount of BG at C/G ratio 3/17 via the electrospinning technique (Ma et al. 2014)

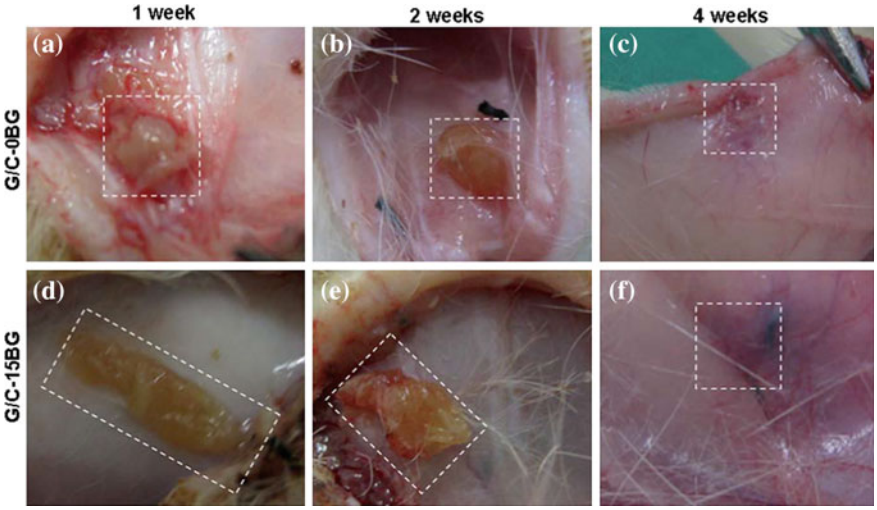

Fig. 9.9 Wound healing upon implanting G/C-xBG in subcutaneous tissue of rats (Ma et al. 2014)

can be due to two aspects: the release of inorganic ion products via BG dissolution and beneficial G/C functions on the wound site. Due to these two factors, the cellular signaling gets improved and at the same time nanofibrous network

containing BG provides modified surface properties and anti-bacterial activities, which prove beneficial for the anti-adhesion on wet wounds.

Cong and coworkers used Yunnan Baiyao (YB), a well-known Chinese herbal medicine as hemostatic agent, and 45S5 Bioglass® on the diabetic wound healing in diabetic rats. Yunnan Baiyao can cause release of platelet constituents along with enhancing surface glycoprotein's expression on platelets under stimulated conditions which cause shortening clotting/bleeding times in rabbits and rats. The rats were separated into eight groups as shown in Table 9.1.

Figure 9.10 gives the observation after 7, 14, and 21 days for the wounds treated with different methods. After 7 days of treatment, except for the groups 5 and 7, the red granulation tissue has filled up all the wounds. For all the groups, wounds were regularly shaped with rough surface in all groups. Slight enlargement of skin tissue could be seen in all the diabetic groups. After 14 days, all groups showed considerable reduction in wound size, particularly for group I and group VI. Compared with day 7, the edge of wounds was much normal and the inflammatory reaction disappeared. After 21 days, the wounds could be seen covered by new epidermis and showed healing in the groups 1 and 6. For the groups 2 and 3, still open wounds could be seen. The bioactive glass and Yunnan Baiyao ointments have healing

Table 9.1 Coding of experimental animal rats with wounds

	CODES	Ointment	Method of treatment
Each group with 15	1		Non-diabetic saline-treated rat
	2		Saline treated
	3		Vaseline treated
	4	84 % Vaseline + YB	Ointment V treated
	5	84 %Vaseline + 45S5 ointment	Ointment I treated
Rates	6	5 % YB	Ointment II treated
	7	10 % YB	Ointment III treated
	8	20 % YB	Ointment IV treated

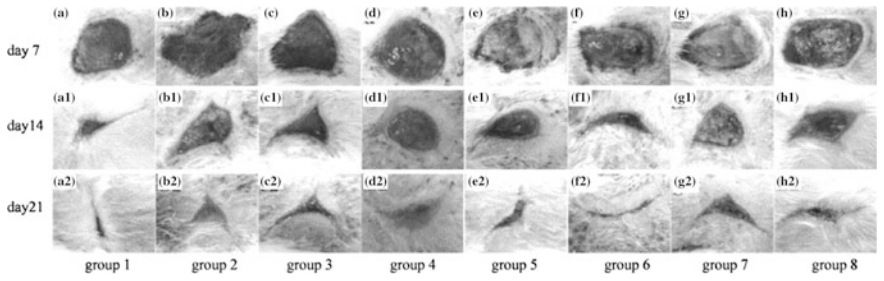

Fig. 9.10 Wound healing in the rat groups using different ointments (Cong et al. 2014)

effects on wounds in diabetic rats. Group 6 containing 5 % Yunnan Baiyao had better results than any other ointment. Diabetic wounds are much more complicated due to neuropathic, vascular, biochemical, and immune function abnormalities. Patients with diabetes have impaired wound healing due to high blood glucose levels. The bioactive glass containing ointments can be better alternatives for curing such diabetic wounds.

Lin and coworkers also worked on producing Vaseline-based ointments with 18 wt% of 58S glass (SGBG-58S), nanoscale BG 58S (NBG-BS), and melt-derived 45S5 glass powders for the treatment of superficial injuries in diabetic rats. The bioactive glass with the ointment and Vaseline were applied directly on the full thickness wounds. Figure 9.11 demonstrates that the wound healing was accelerated in the presence of bioglass, especially SGBG-585, after day 16. In contrast to this, the wounds were still open for the control group, and it took little longer for the healing. Increased proliferation of fibroblast could be seen along with new capillary formation and granulation tissues for the BG-treated ointments, and immunohistochemical assays showed the VEGF presence in all tissues at day 7.

No adverse reaction or inflammatory response could be seen in the animals treated with bioactive glass ointments. Moreover, the wound healing results demonstrated quick healing of wounds with the sol-gel-derived glasses than the melt-quenched 45S5 glass, attributed to the larger surface area of the sol-gel glasses.

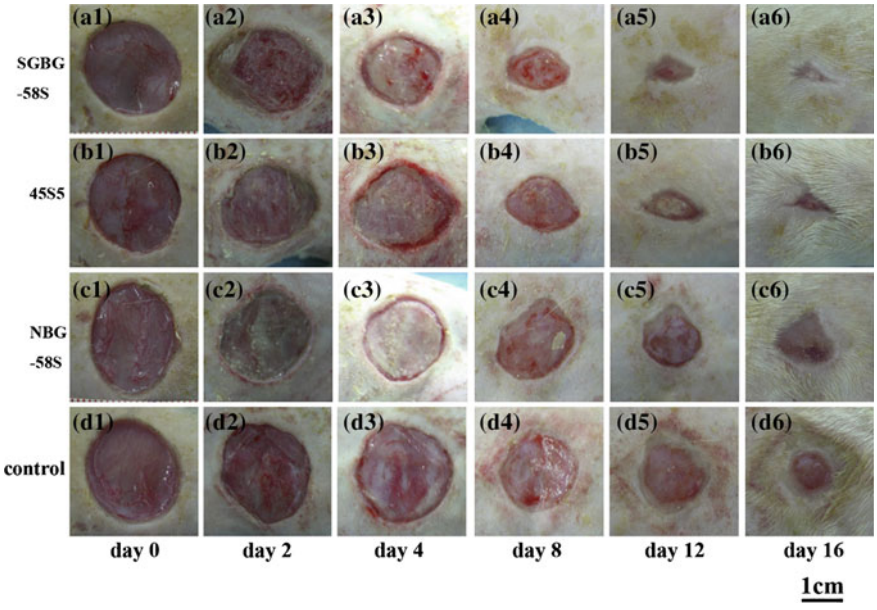

Fig. 9.11 Healing in BG-treated and untreated wounds from days 0–16 (Lin et al. 2012)

Yang and coworkers conducted comprehensive evaluation of HAp conversion and cell–glass interactions under both dynamic and static modes. The nano/microfibers used are of 45S5, 13-93B3, and 1605 [6 % Na_2O, 12 % K_2O, 5 % MgO, 20 % CaO, 4 % P_2O_5, 51.6 % B_2O_3, 0.4 % CuO, 1 % ZnO, wt%) for their effect on wound healing as well on the human fibroblast skin line (CCL-10). The morphology of fibers under a dynamic flow condition with continuous fresh media supply is shown in Fig. 9.12. The fibers possessed smooth surface with fewer fine structures such as flakes and whiskers. The 45S5 fibers had eroded/porous inner structures. For the 13-93B3 fibers, a polished surface morphology with porous granule network underlying the surface layers could be seen. Highly roughened surface and protruded spherical structures could be seen for the borate-based 1605 fibers.

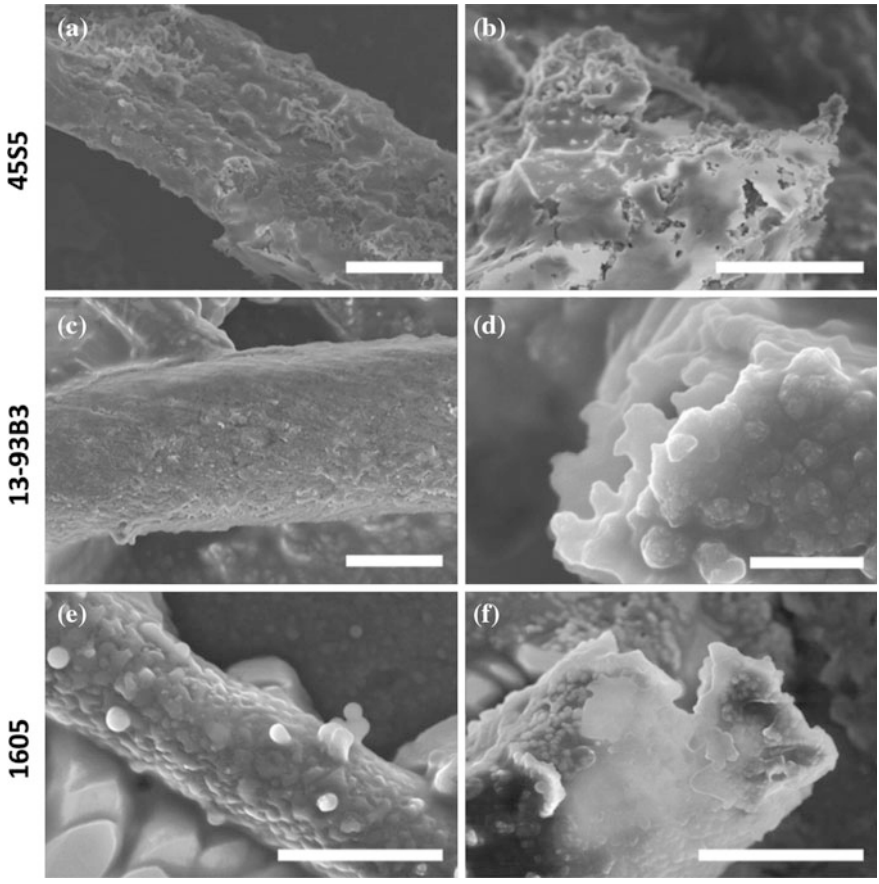

Fig. 9.12 SEM images of **a**, **b** 45S5 **c**, **d** 13-93B and **e**, **f** 1605 bioactive fiber surface and end-face after dynamic-mode soaking in cell culture medium for 5 days (Yang et al. 2015)

Eroded fiber surfaces and hollowed cross section could be seen upon viewing the fibers under high magnification. The fibers had a negative effect on cell viability at high dosages. For 45S5 and 1605 glass, high cell proliferation could be observed for the dosages of ≤ 750 μg/ml and ≤ 250 μg/ml, respectively. The cell viability has been function of both the treatment time and fiber dosage. The fiber dosage <200 μg/ml provided better viability than the control. If the fiber is presoaked with serum-free cell culture medium, then cell proliferation got stimulated by 35–40 % by 45S5 and 13-93B3, even after 1-h soaking. The cytotoxicity could be reduced by the partial conversion of fibers, attributed to the rapid refreshing rate of dissolved calcium and boron, along with improved surface elemental deposition. Higher cell viabilities could be seen for the fiber groups with dynamic control group as compared to the static control. Though silicate 45S5 fibers have wider dosage range for positive cell proliferation, but borate-based fiber can stimulate higher cell viabilities than the silicate glass fibers. Under static mode, negative impact on the cell migration was observed in all fiber-treated groups, with higher impairment effects caused by the borate glasses. The formation of new tissue around the wound is characterized by cell migration and keratinocyte/fibroblasts proliferation. The tissue repairing mechanism could be seen by 45S5, 13-93B3 and 1605, along with the fiber-stimulating effect on cell proliferation and migration abilities.

Gillette and coworkers applied BG with particulate <20 μm into surgically made open wounds in nine dogs. The wounds made were bilateral, so that the BG-treated wound and control could be studied together. Small slurry of BG and blood was produced, which was then applied to the wounds. A small amount of this paste lied between the wounds edges, whereas most of the mixture stayed in the subcutaneous area of the wound. After 5 days of application, no significant difference could be observed in the breaking strength of healed skin in all the samples, but increase in breaking strength of healed cutaneous/subcutaneous trunci in treated wounds could be seen as compared to control wounds. In addition to this, no inflammatory response of the host tissue could be seen.

Wray worked on repairing the wounds on small scale for worst-case diabetic patients using 13-93B3 glass nanofibers ranging from 5 μm to 300 nm. Accelerated healing of the wounds could be observed along with marked decrease in scar tissue formation as compared to congenitally treated wounds. Silver-containing nanoporous bioactive glass (n-BGS) has been investigated for its anti-bacterial dressings and hemostatic properties compared to the bioactive glass without nanopores (BGS). n-BGS possesses higher surface area compared to the BGS, resulting in its higher water absorption efficacy. n-BGS released Ag^+ ions rapidly, though the concentration of silver in solution was same after 24 h of incubation in phosphate-buffered solution (PBS). For n-BGS at 0.02 wt% silver concentration, highest anti-bacterial rate of 99 % could be obtained for the Escherichia coli, after 12-h incubation time. n-BGS and BGS particles were applied to the damaged femoral arteries and veins of male New Zealand white rabbits. n-BGS has significantly lower clotting times in both prothrombine time (PT) and activated partial

thromboplastin time (APTT) in vitro. Hence, silver-doped n-BGS accelerates clotting, provides bactericidal effect, and promotes hemorrhage control.

Zhao and coworkers fabricated wound dressings comprising of copper doping (0–3 wt% CuO) in the 13-93B3 microfibers. Copper is considered to be an essential component of angiogenic response as they stabilize the expression of hypoxia-inducible factor (HIF-1α), mimicking hypoxia and hence playing a crucial role in the recruitment and differentiation of the cells as well as blood vessel formation. Cu^{2+} release also stimulates the expression of proangiogenic factors such as transforming growth factor-β (TGF-β). Cu^{2+} ions enhance implant vascularization when used in combination with the VEGF and bFGF. It was observed that after 7 days of cell culture, Cu-doped microfibers proliferated HUVEC better than the cell cultured on the ionic dissolution product of undoped microfibers. HUVEC incubated with the ionic dissolution product of Cu-doped microfibers yielded elongated and tube-like structures (after incubating on the matrigel substratum for 12 h). Anyhow, incomplete or sparse tubular network formation could be seen, when HUVECs are treated with the ionic dissolution product of undoped microfibers. VEGF, bFGF, and PDGF gene expressions for fibroblasts incubated in the ionic dissolution products of microfibers enhanced as the content of CuO increased in fibers, indicating the proangiogenic potential of the bioactive glass microfibers. The wound images with the application of Cu-doped 13-93B3 are shown in Fig. 9.13 at 0, 6, 10, and 14 days.

The smallest wound size was observed in the 3Cu-BG group though the wound size decreased with the healing time for all the groups. The wound closed by day 14, upon its treatment with 3Cu-BG. For the quantification of wound, following equation is used.

$$\% \text{ Wound size reduction} = [(A_o - A_t)/A_o] \times 100 \tag{9.1}$$

where A_o and A_t are wound areas initially and at each time point. The micro-CT showed a high number density of blood vessels in the defects treated with 3Cu–BG microfibers than the untreated or BG microfiber-treated wounds. Histological analysis of Masson's trichrome-stained section of the three treatment groups is shown as in Fig. 9.14.

Extensive collagen deposition and thick wavy collagen fibers could be observed in wound areas treated with BG microfibers as compared to the untreated defects. The 3Cu-BG microfibers treated wound showed highest collagen fibers arranged in an orderly fashion similar to the normal skin. For both 3Cu-BG and BG, the accelerated formation of hair follicles and sebaceous glands, 14 days postsurgery, could be obtained. Together, all these results indicated that the Cu-doped borate bioactive glass microfibers are promising candidates for wound dressing.

Li and coworkers studied the wound healing treatment using Bioglass® by affecting gap function connexin 43 mediated endothelial cell behavior. All the endothelial cell behaviors are related to gap junctional cell-to-cell communications

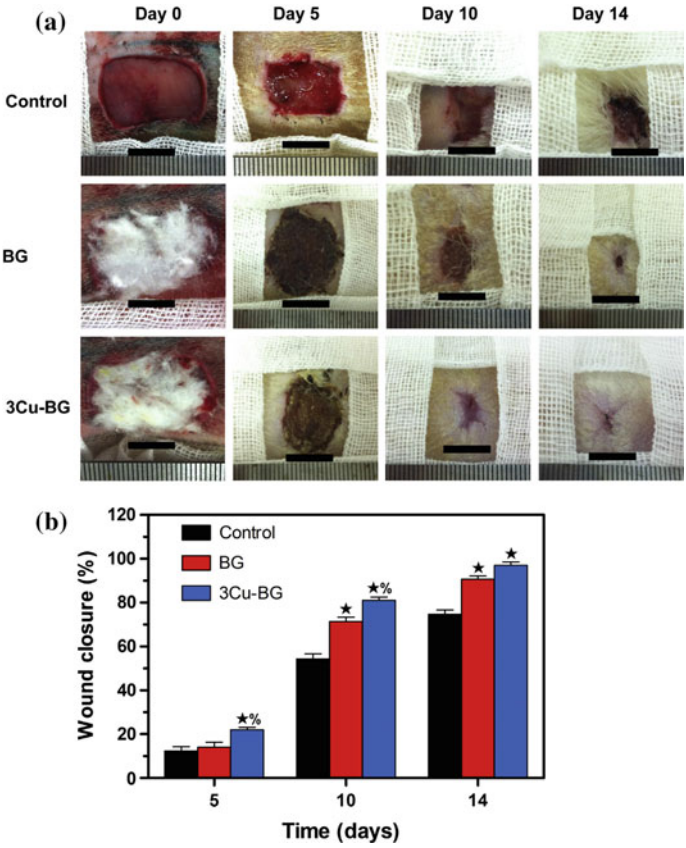

Fig. 9.13 **a** Skin defects in rodents, left untreated (control) or treated with the BG or 3Cu-BG microfibers, at 0, 5, 10, and 14 days postsurgery. **b** Percent wound closure for the untreated defects (control) and the defects treated with the BG or 3Cu-BG microfibers at 5, 10, and 14 days postsurgery (Zhao et al. 2015)

as connexin 43 (C × 43) plays imperative role in determining the fate of endothelial cell along with cell-to-cell communication mercenary for angiogenesis and wound heating. C × 43 is the most ubiquitous connexins in skin located in dermal appendages, fibroblasts as well as cutaneous vasculature. C × 43 anti-sense C × 43 mimetic peptides and C × 43 hemichannels play an important role in the wound healing. The 45S5 BG extracts were diluted in endothelial cell medium at ratios of 1/8, 1/16, 1/32, 1/64, 1/128, 1/256, and 1/512. For BG 1/8 and BG 1/16, the proliferation of HUVEC is suppressed as compared to the medium alone. Under hypoxia conditions, almost 80 % of HUVEC cultured in BG 1/128 ion extracts remained viable and the survival was same as that of the non-hypoxic conditions. For BG 1/152, only 65 % cells remain alive, indicating that BG at appropriate

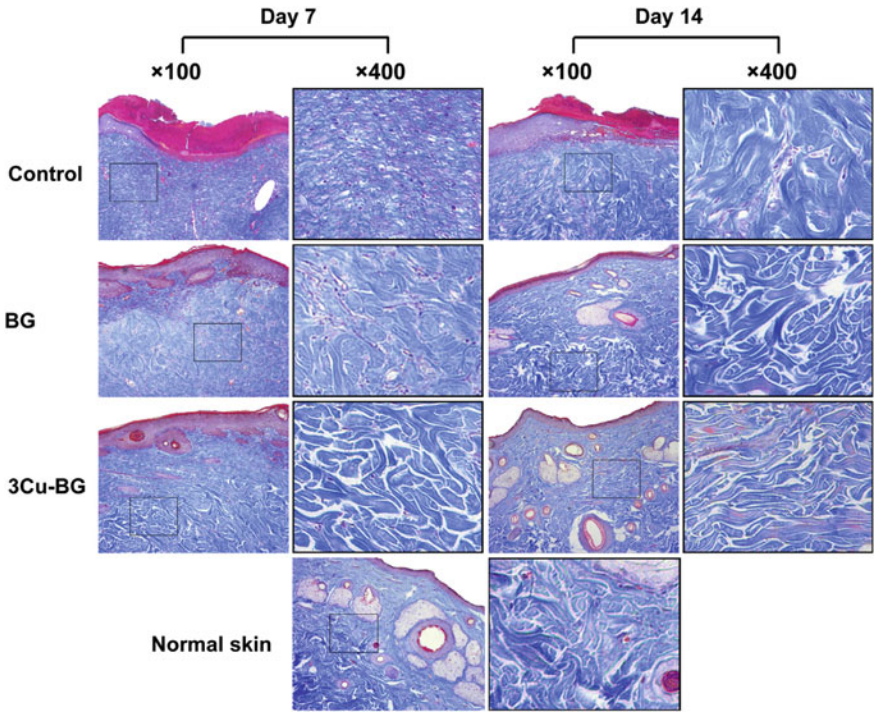

Fig. 9.14 Masson's trichrome-stained sections of the untreated defects (control) and the defects treated with the BG or 3Cu-BG microfibers at 7 and 14 days postsurgery, indicating collagen deposition (Zhao et al. 2015)

concentration could protect HUVECs exposed to hypoxic conditions. After 1-day culture in HUVEC, the culture media containing BG 1/64, BG 1/128, and BG 1/256 upregulated the bFGF, VEGF, and KDR gene expression. After 7 days, the VEGF and KDR expressions in HUVECs are shown as in Fig. 9.15.

Immunofluorescence staining yielded more positive results for in KDR HUVECs cultured in BG 1/64, BG 1/128, and BG 1/256 than the cell cultures in BG 1/32 and BG/512. The KDR expression in HUVECs cultured with BG 1/64, BG 1/128, and BG 1/256 is higher than the control results. C × 43 expression in HUVECs cultured in BG 1/64 and BG 1/128 for 7 days is much higher than the cells cultured in endothelial medium alone BG 1/32, BG 1/512. For the wound treated with BG, the granulation tissue formation could be seen in the form of vascularized endodermis (beginning day 6). After 12 days, the granulation tissue is much more organized, but no neoepidermis formation could be seen for the untreated wound though eschar and noticeable granulation tissue formation could be seen. Figure 9.15 gives the immunolabeling of C × 43 in wound sites at days 2 and 12. C × 43 expression could be seen after 2 days of operation in control and BG-treated wounds. After 12 days of operation, highest C × 43 expression could

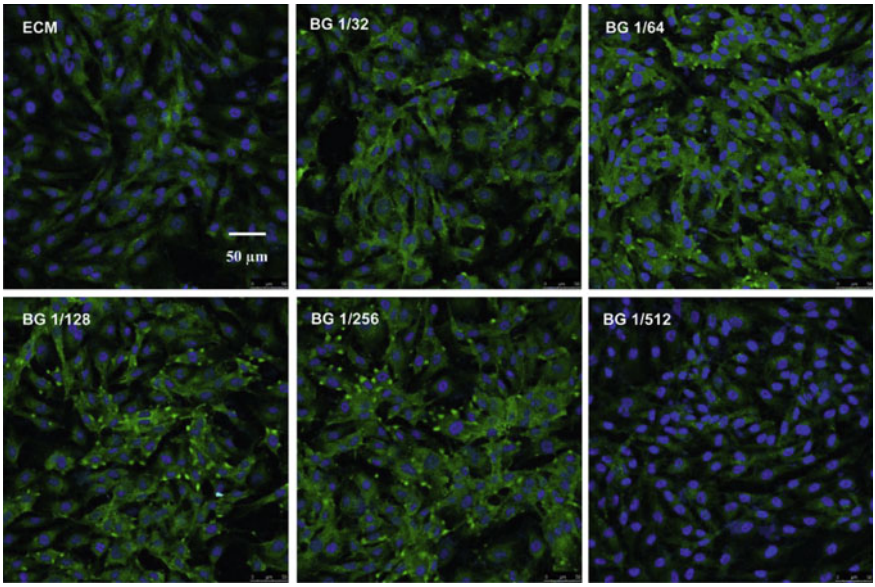

Fig. 9.15 KDR protein expression and localization in HUVECs cultured with different media for 3 days (Li et al. 2016)

be seen for the BG-treated wounds than the untreated ones. Hence, the results can be summed up as:

- BG protects endothelial cells by reducing open probability of hemichannels during the early stages of wound healing during which hypoxia can occur.
- During the cell migration and proliferation, BG stimulates endothelial cells to migrate into wound bed and upregulate VEGF from the existing endothelial cells.
- Gap junctional communication between endothelial cells is increased, once the endothelial cells reach at the wound bed, thereby stimulating vascularization.

Rai and coworkers fabricated poly (3-hydrony-octanoate) composite forms with nanosized bioactive glass (nBG) for the wound dressings. With increasing proportion of glass nanoparticles, the toughness is increased with enhanced polymer wettability along with decreased clothing time of citrated whole blood. Increased cell proliferation could be seen when human keratinocytes were cultured on the composite films attributed to the increased surface area of the nBG.

Bibliography

Li H, He J, Yu H, Green CR, Chang J (2016) Bioglass promotes wound healing by affecting gap junction connexin 43 mediated endothelial cell behavior. Biomaterials 84:64–75. doi:10.1016/j.biomaterials.2016.01.033

Ma W, Yang X, Ma L, Wang X, Zhang L, Yang G, Gou Z (2014). Fabrication of bioactive glass-introduced nanofibrous membranes with multifunctions for potential wound dressing. RSC Adv 4(104):60114–60122. doi:10.1039/C4RA10232K

Day RM (2005) Bioactive glass stimulates the secretion of angiogenic growth factors and angiogenesis in vitro. Tissue Engineering 11(5):768–777. doi:10.1089/ten.2005.11.768

Yang Q, Chen S, Shi H, Xiao H, Ma Y (2015) In vitro study of improved wound-healing effect of bioactive borate-based glass nano-/micro-fibers. Materials Science and Engineering C 55:105–117. doi:10.1016/j.msec.2015.05.049

Zhao S, Li L, Wang H, Zhang Y, Cheng X, Zhou N, Zhang C (2015) Wound dressings composed of copper-doped borate bioactive glass microfibers stimulate angiogenesis and heal full-thickness skin defects in a rodent model. Biomaterials 53:379–391. doi:10.1016/j.biomaterials.2015.02.112

Kent Leach J, Kaigler D, Wang Z, Krebsbach PH, Mooney DJ (2006) Coating of VEGF-releasing scaffolds with bioactive glass for angiogenesis and bone regeneration. Biomaterials 27 (17):3249–3255. doi:10.1016/j.biomaterials.2006.01.033

Lin C, MaO C, Jhang J, Li Y, Chen X (2012) Healing effect of bioactive glass moment on full thickness skin wounds. Biomed Mater 7(4):045017

Haro Durand LA, Vargas GE, Romero NM Vera-Mesones R, Porto-López JM, Boccaccini AR, Gorustovich A (2015) Angiogenic effects of ionic dissolution products released from a boron-doped 45S5 bioactive glass. J Mater Chem B 3(6):1142–1148. doi:10.1039/C4TB01840K

Cong M, Lin C, Chen X (2014) Enhanced healing of full-thickness diabetic wounds using bioactive glass and Yunnan baiyao ointments. J Wuhan Univ Tech, Mater Sci Ed 29(5):1063–1070. doi:10.1007/s11595-014-1044-y

Fujibayashi S, Neo M, Kim HM, Kokubo T, Nakamura T (2003) Biomaterials 24:1349–1356

Wilson J, GH Pigott, FJ Schoen, LL Hench (1981) J Biomed Mater Res 15(6):805–817

Gatti aM, Valdrè G, Andersson OH (1994) Analysis of the in vivo reactions of a bioactive glass in soft and hard tissue. Biomaterials 15(3):208–212

Murphy WL, Simmons CA, Kaigler D, Moona DJ (2004) J Den Res 83:204–210

Aina V, Malavasi G, Pla AF, Munaron L, Morterra C (2009) Zinc-containing bioactive glasses: surface reactivity and behaviour towards endothelial cells. Acta Biomater 5:1211–1222

Leu A Leach JK (2008) Pharn Res 25:1222

Lin Y, Brown RF, Jung SB, Day DE (2014) J Biomed Mater Res A 102:4491–4499

Mahmood J, Takita H, Ojima Y, kobayshi M, Kohgo T, Kubole Y (2001) J Biochem 129:163

Ghosh SK, Nandi SR, Rumdu B, Datta S, De DK, Roy SR, Baseu D (2008) J Biomed Mater Res Part B 86:217

Nandi SK, Kundu B, Datta S, De DK, Basu D (2009) Res Vet Sci 86:162

Andrade AL, Andrade SP, Domingues RZ (2006) J Biomed Mater Res B 79:122

Gerhardt L-C, Widdows KL, Erol MM, Burch CW, Sanz-Herrera JA, Ochoa I et al (2011) The pro-angiogenic properties of multi-functional bioactive glass composite scaffolds. Biomaterials 32(17):4096–4108

Gillette RL, Swaim SF, Sartin EA, Bradley DM, Coolman SL (2001) Am J Vet Res 62(7):1149–1153

Wray P (2011) Am Ceram Sec Bull pp 25–29

Hu G, Xiao L, Tong P, Bi D, Wang H, Ma H (2012) Int J Nauomedicine 7:2613–2620

Rai R, Boccaccini AR (2010) ATP Conf Proc 1255:126–128

Baino F, Novajra G, Miguez-Pacheco V, Boccaccini AR, Vitale-Brovarone C (2016) Bioactive glasses: special applications outside the skeletal system. J Non-Cryst Solids 432:15–30. doi:10.1016/j.jnoncrysol.2015.02.015

Krishnan V, Lakshmi T (2013) Bioglass: a novel biocompatible innovation. J Adv Pharm Tech Res 4(2):78–83. doi:10.4103/2231-4040.111523

Nganga S (2013) Glass-Fiber reinforced cpmposite for bone implants. Evaluation of antimicrobial effect and implant fixation

Tobergte DR, Curtis S (2013) No title no title, vol 53. J Chem Inf Model. doi:10.1017/CBO9781107415324.004

Fujibayashi S, Neo M, Kim H-M, Kokubo T, Nakamura T (2003) A comparative study between in vivo bone ingrowth and in vitro apatite formation on Na_2O-CaO-SiO_2 glasses. Biomaterials 24(8):1349–1356. doi:10.1016/S0142-9612(02)00511-2

Khader B, Curran D, Peel S, Towler M (2016) Glass polyalkenoate cements designed for cranioplasty applications: an evaluation of their physical and mechanical properties. J Funct Biomater 7(2):8. doi:10.3390/jfb7020008

Gorustovich, AA Roether JA, Boccaccini AR (2010) Effect of bioactive glasses on angiogenesis: a review of in vitro and in vivo evidences. Tissue Eng Part B Rev 16(2):199–207. doi:10.1089/ten.TEB.2009.0416

Keshaw H, Forbes A, Day RM (2005) Release of angiogenic growth factors from cells encapsulated in alginate beads with bioactive glass. Biomaterials 26(19):4171–4179. doi:10.1016/j.biomaterials.2004.10.021

Kiefer K, Amlung M, Aktas OC, De Oliveira PW, Abdul-Khaliq H (2016) Novel glass-like coatings for cardiovascular implant application: preparation, characterization and cellular interaction. Mater Sci Eng C 58:812–816. doi:10.1016/j.msec.2015.09.063

Kokubo T (1991) Bioactive glass ceramics: properties and applications. Biomaterials 12(2):155–163. doi:10.1016/0142-9612(91)90194-F.

Miguez-pacheco V, Greenspan D (2015) Bioactive glasses in soft tissue repair. American Ceram Soc Bull 94(6):27–31. Accessed from http://ceramics.org/wp-content/uploads/2009/06/Aug_Feature.pdf

Miguez-Pacheco V, Hench LL, Boccaccini AR (2015) Bioactive glasses beyond bone and teeth: emerging applications in contact with soft tissues. Acta Biomater 13:1–15. doi:10.1016/j.actbio.2014.11.004